Design, Synthesis, and Imaging of an Activatable Photoacoustic Probe

6 AUTHORS, INCLUDING:

Jelena Levi
Stanford University
19 PUBLICATIONS **1,261** CITATIONS

SEE PROFILE

Te Jen Ma
Marvell Technology Group
11 PUBLICATIONS **632** CITATIONS

SEE PROFILE

Pierre T Khuri-Yakub
Stanford University
570 PUBLICATIONS **8,717** CITATIONS

SEE PROFILE

Design, Synthesis and Imaging of an Activatable Photoacoustic Probe

Jelena Levi[†], **Sri Rajasekhar Kothapalli**[‡], **Te-Jen Ma**[§], **Keith Hartman**[‡], **Butrus T. Khuri-Yakub**[§], and **Sanjiv Sam Gambhir**[*,‡,†]

Canary Center at Stanford for Cancer Early Detection, 1501 S California Avenue, Palo Alto, 94305, Molecular Imaging Program at Stanford, Department of Radiology and Bio-X Program, Stanford University, Palo Alto, California 94305 and Department of Electrical Engineering, Stanford University, Palo Alto, California 94305, USA

Abstract

Photoacoustic tomography is a rapidly growing imaging modality that can provide images of high spatial resolution and high contrast at depths up to 5 cm. We report here the design, synthesis and evaluation of an activatable probe that shows great promise in enabling detection of the cleaved probe in the presence of the high levels of non-activated, un-cleaved probe, a difficult task to attain in absorbance-based modality. Before the cleavage by its target, proteolytic enzyme MMP-2, the probe, an activatable cell penetrating peptide, Ceeee[Ahx]PLGLAGrrrrrK, labeled with two chromophores, BHQ3 and Alexa750, shows photoacoustic signal of similar intensity at the two wavelengths corresponding to the absorption maxima of the chromophores, 675 and 750 nm. Subtraction of the images taken at these two wavelengths makes the probe effectively photoacoustically silent as the signals at these two wavelengths essentially cancel out. After the cleavage, the dye associated with the cell penetrating part of the probe(CPP), BHQ3, accumulates in the cells, while the other dye diffuses away, resulting in photoacoustic signal seen only at one of the wavelengths, 675 nm. The subtraction of the photoacoustic images at two wavelengths reveals the location of the cleaved (activated) probe. In the search for the chromophores that are best suited for photoacoustic imaging we have investigated photoacoustic signal of five chromophores absorbing in the NIR region. We have found that the photoacoustic signal did not correlate with the absorbance and fluorescence of the molecules, as the highest photoacoustic signal arose from the least absorbing quenchers BHQ3 and QXL 680.

Introduction

Biomedical imaging has been revolutionized by the field of molecular imaging that offers the possibility of understanding diseases at the molecular level[1,2]. Photoacoustic tomography, a rapidly growing imaging technique, combines optical and ultrasound imaging in such a way that the result is a modality with characteristics superior to each of the component imaging techniques[3,4]. As a molecular imaging modality that offers both high spatial resolution and high contrast, photoacoustic tomography utilizes endogenous[4,5] as well as exogenous[6–8] light absorbers as entities providing the optical contrast in biological

[*]sgambhir@stanford.edu .
[†]Canary Center at Stanford for Cancer Early Detection
[‡]Molecular Imaging Program at Stanford, Department of Radiology and Bio-X Program, Stanford University
[§]Department of Electrical Engineering, Stanford University

tissues. However, probes that show signal only in the presence of a specific target, so called activatable or smart probes, have not yet been reported for photoacoustic imaging. Activatable probes for optical and magnetic resonance imaging have been extensively studied and applied for *in vivo* imaging[9–14]. They show superior specificity and sensitivity to the probes that provide signal regardless of interaction of probe with the target. Here, we wish to report the design and evaluation of a photoacoustic smart probe that provides a target dependant photoacoustic signal and enables visualization of the signal only in the presence of the target of interest.

Dual and multi-wavelength photoacoustic imaging have been employed in acquiring impressive images with clearly distinguished endogenous molecule-specific signals[15–18]. We designed our probes wanting to take advantage of dual wavelength imaging (Figure 1). In the intact state, the probe should show photoacoustic signal at the two wavelengths that correspond to the absorption maxima of the two chromophores within the probe. When the probe is cleaved by the appropriate enzyme, the dye associated with the cell penetrating part of the probe (CPP) accumulates in nearby cells, while the other dye component diffuses away. Photoacoustic signal is thus expected only at the absorption wavelength of the dye accumulated in the cells. The main criteria for choosing the chromophores were high absorption in the near infra-red (NIR) region and well separated, mutually non-overlapping, absorption spectra. The probes were designed to be specific for an extensively studied target, matrix metalloprotease 2 (MMP-2), a protease found to be over-expressed in many cancers and associated with tumor aggressiveness[19,20]. Activatable cell penetrating peptide (ACPP) was selected as the probes' peptide platform because of its proven efficacy in detecting MMP-2, both *in vitro* and in mouse models[21,22]. ACPP has the MMP-2 cleavable amino acid sequence between polyarginine based cationic (CPP) and polyanionic domains. We hypothesized that the hairpin structure[22] of ACPPs would allow the interaction between the two dyes resulting in either resonance energy transfer or static quenching, both of which could lead to a target-dependant photoacoustic probe. The peptide sequence used in our study, Ceeee[Ahx]PLGLAGrrrrrK, differs from the one reported by Jiang et. al.[22] in the number of arginine and glutamic acid residues. The number of these amino acids is important for the transduction efficiency of the polyarginine sequence[23,24]. We have chosen the shortest polyarginine sequence shown to provide efficient cargo delivery to facilitate the separation of the charged parts of the peptide after enzymatic cleavage.

Results and Discussion

Chromophore selection

We investigated the photoacoustic signal intensity for the five chromophores that met the criteria of high NIR absorption and mutually non-overlapping absorption spectra. Two of those were quenchers, BHQ3 and QXL680, and three were fluorophores, Cy5.5, Alexa750 and Hilyte750. As seen in Figure 2, the strongest signal was observed for the two quenchers, QXL680 and BHQ3. Taking into account only extinction coefficients and quantum yields of the chromophores (Table 1), one would predict that all three fluorescent molecules would give stronger photoacoustic signal than the less absorbing quenchers. However, this result indicates that besides absorbance and fluorescence there are other processes that contribute to and affect the photoacoustic signal of a molecule. Kinetics of non-radiative deactivation, triplet state contribution and photobleaching are only some of the processes that need to be considered when determining a molecule's ability to convert light energy into heat and thus its photoacoustic signal[25,26]. The parameter that describes proportionality between absorbed light energy and photoacoutic pressure, called Grüneisen coefficient[27], could also be used to explain the photoacoustic behaviour of different molecules. Although the studies investigating Grüneisen coefficient of tissues and certain materials have been published, no such studies have been reported for the molecules such as chromophores. For a majority of

the molecules the parameters determining the photoacoustic properties are not known or are not readily accessible and molecules' photoacoustic behavior likely needs to be determined empirically.

Synthesis of the probes and their spectral characterization

For a probe to produce a strong photoacoustic signal in the cleaved state, the part of the probe that is able to penetrate the cell wall and accumulate in the cells after the cleavage needed to be labeled with a chromophore that shows the greatest photoacoustic signal. Therefore, we designed our probes to have the two quenchers found to have the strongest photoacoustic signal attached to the cell penetrating part of the probe, and the fluorophores conjugated to the opposite end of the peptide chain. The dyes were conjugated to the peptide in one step through Lysine and Cysteine (Figure 3). Four dual labeled probes were synthesized. Two probes that were designed to be activatable photoacoustic probes (APP), BHQ3-APP-Alexa750 (B-APP-A) and QXL680-APP-Hilyte750 (Q-APP-H), each have an ACPP platform and are expected to show MMP-2 specific accumulation (Figure 3a). To demonstrate the capability of our two wavelength approach in distinguishing between specific and high non-specific accumulation of the probe, we have synthesized two photoacoustic probes (PP), BHQ3-PP-Alexa750 (B-PP-A) and QXL680-PP-Hilyte750 (Q-PP-H), designed to accumulate in the cells independent of the presence of MMP-2. These two probes lack the polyanionic domain of the APP and are expected to enable the delivery of both chromophores into the cell (Figure 3b) thus describing the situation of nonspecific uptake and lack of clearance of the intact probe in eventual *in vivo* application.

All dual labeled probes showed absorbance spectra suggestive of intramolecular chromophore dimerization (Figure 4 a, c). Dimerization of the chromophores is known to lead to the probes with absorption spectra that are not a sum of the components' absorption spectra, as observed in Föster resonance energy transfer (FRET), but rather a non-linear spectral combination of the two dyes as seen in static quenching[29–31]. Static quenching was proposed as a dominant interaction for certain chromophore pairs, characterized by the formation of the ground state complex with distinct absorption spectrum, non reflective of the extinction coefficients of the component chromophores. Fluorescence measurements offered further evidence for static quenching through formation of dimers. Despite the lack of spectral overlap between the fluorophores and the quenchers, emission intensity of the probes was drastically decreased compared to those of the fluorophores (Figure 4b, d). The dimer formation and properties of the choromophores capable of forming them have been the subject of many studies.[29,30,32,33] Electronic and steric factors, symmetry and hydrophobicity are some of the characteristics that are important for the chromofores' tendency to dimerize. Although the hairpin structure of the ACPPs brings chromophores at a close distance and can contribute to their dimerization, we believe that it was not a determining factor in these probes. This is evident from the absorbance spectra of the probes lacking the hairpin structure (Figure 4a, c dashed lines). In these probes, too, dimerization led to the formation of ground state complexes with distinct spectral properties.

Photoacoustic imaging of the enzymatic cleavage

The in vitro cleavage of the B-APP-A probe by MMP-2 led to the separation of the chromophores and consequently to the change in the absorption (Figure 5a) and fluorescence spectrum (Supporting information). While the absorption corresponding to Alexa750 remained the same, a significant decrease in absorption was observed in the blue shifted region. On the other hand, the photoacoustic signal detected at 675 nm (Figure 5b) after the cleavage was slightly higher than the one observed at 750 nm (Figure 5c). These results can be explained by the difference in properties between the heterodimer that exists before the cleavage and the monomeric chromophores after the cleavage. As mentioned

earlier, the probe in its intact state shows properties indicative of the heterodimer with spectral and photoacoustic properties that do not represent a linear combination of the component chromophores (Figure 4). After the cleavage, the dimer is separated into the individual chromophores and the absorption as well as the photoacoustic signal are reflective of the properties of the individual chromphores (Table 1, Figure 2).

The in vitro cleavage results do not provide a proper test of the probe's ability to provide target specific signal, as they do not take into account the accumulation of one chromophore and diffusion of the other after enzyme mediated cleavage. The full potential of the probes in combination with the two wavelength approach was revealed by comparing the photoacoustic signal of the intact probe to the photoacoustic signal of the cell penetrating part of the cleaved probe carrying one of the chromophores (Figure 6). Of the two probes B-APP-A showed superior characteristics for dual wavelength imaging. A high photoacoustic signal for the uncleaved probe was observed at both 675 nm and 750 nm, while cleaved probe showed signal exclusively at 675 nm. What makes this probe especially useful is the fact that the signals observed for the intact probe at two wavelengths are of comparable intensity. Normalized subtraction of the two images, led to a new image that shows signal only for the cleaved probe (Figure 6c). The other probe, Q-APP-H, showed signal at both wavelengths as well, but the two were not of similar intensity. Consequently, the subtraction of the images led to an image that shows a drop in the photoacoustic signal for the cleaved probe (Figure 5f). Clearly, of the two probes, B-APP-A shows greater potential as an activatable photoacoustic probe.

Photoacoustic imaging of the probes' accumulation in cells

To further demonstrate the value of our approach toward smart photoacoustic probes, we incubated fibrosarcoma cells, HT1080, with three probes: un-cleaved, MMP-2 specific probe, B-APP-A; un-cleaved, MMP-2 non-specific probe, B-PP-A; and cleaved probe (CP), BHQ3-CP. MMP-2 is an extracellular enzyme and its secretion by HT1080 cells has been determined in the concentrated growth medium by zymography (Supporting Information). However, we expected only negligible cleavage to occur in cell culture due to the dilution of the enzyme in the medium[34]. To the best of our knowledge, cleavage of any probe by MMP-2 in cell culture has not been reported to date. The use of purified MMP-2 enzyme in vitro requires the activation of the enzyme by 4-aminophenylmercuric acetate (APMA)[35]. It is thought that APMA disrupts the complex between Cys_{73} in the propeptide domain and zinc atom in the active site of the enzyme. The disruption of this complex leads to autolytic cleavage of the propeptide domain and activation of the enzyme[36]. Instead of pre-cleaving the probe with the activated MMP-2 in vitro that requires the use of a mercuric compound that would be toxic to the cells, we have synthesized the expected product of the cleavage reaction (see Supporting Information), B-CP and used it for cell incubation.

As mentioned earlier, because it has a polyanionic domain that prevents the entrance of the probe, B-APP-A is expected to show low cell accumulation, while B-PP-A and B-CP probes, lacking the polyanionic counterpart to the cell penetrating peptide, are anticipated to accumulate in cells to a much larger extent. As expected, no photoacoustic signal was observed at either wavelength for cells exposed to B-APP-A probe. A control fluorescence image confirmed a low level of accumulation of the probe (Figure 7a). The non-specific accumulation, illustrated by using B-PP-A, on the contrary, showed high signal at both wavelengths (Figure 7b, c). Because the signals at these two wavelengths are of similar intensity the subtraction image (Figure 7d) shows minimal signal coming from the accumulation of B-PP-A. In other words, the subtraction of the images makes the un-cleaved probe effectively photoacoustically silent. Because the signals at two wavelengths for non-activated, un-cleaved probe cancel out, the decrease in signal after cleavage of the probe, as observed in Figure 5, should not pose a problem in identifying the location of MMP-2

activity. Importantly, the uptake of the cleaved probe indicated by photoacoustic signal at 675 nm was clearly distinguished from the uptake of both intact probes by subtraction of the images at two wavelengths (Figure 7d). Taken together, these results indicate that by using a dual wavelength imaging in combination with our activatable photoacoustic probe, B-APP-A, it is possible to isolate low levels of target specific signal from high levels of non-activated probe, a challenging task to attain in an absorbance-based modality.

In this study we used a limited number of chromophores and chromophore combinations suitable for use in activatable photoacoustic probes. In future studies we plan to explore other combinations as well as investigate the optimal number of arginines for the most efficient MMP-2-specific delivery of the chromophores.

Conclusion

We report here an activatable photoacoustic probe visualized by utilizing two wavelength imaging. The combination of the intramolecular dimer as a probe and dual wavelength imaging offers a versatile, generalizable approach to a target dependant photoacoustic probe. By changing chromophores and peptide backbone, the probe can be tailored to the target protease as well as to the imaging window. In addition, this method is adaptable to applications in living subjects as probes carry chromophores that can be clearly distinguished from the highly absorbing biomolecules, such as hemoglobin, using newly developed techniques and instruments[37,38]. Because it offers highly specific photoacoustic images, this method could prove useful in pre-clinical models, photoacoustic guided surgical interventions, diagnostics, treatment efficacy evaluations, as well as many other applications.

Experimental section

Probe synthesis and characterization

About 300 μg peptides were dissolved in 200 μl PBS (pH 7.4). To that solution were added 300 μl of N-hydroxysuccimide ester dye (1mg/1mL DMF solution) followed by 300 μL maleimide dye (1mg/1mL DMF solution). After 2 hours, the reaction mixture was centrifuged to remove any insoluble materials and the supernatant injected onto HPLC column. Products were collected, lyophilized and characterized by MALDI or ESI. Peptides used for conjugation had the following sequences: Ac-CeeeeXPLGLAGrrrrrKCONH2 (abbreviated as APP); Ac-CGVRPLKrrrrr (abbreviated as PP) and Ac-LAGrrrrrK (abbreviated as CP). Small letters denote D-amino acids and X signifies 6-aminohexanoyl acid. BHQ3 and QXL680 were in the form of the NHS ester and Alexa750 and Hilyte750 had maleimide as a functional group. Four dual labeled probes were synthesized: B-APP-A (Alexa750-Ac-Ceeee[Ahx]PLGLAGrrrrrK-CONH2-BHQ3)-retention time 16.7 min; ESI+ 3787.0; B-PP-A (Alexa750-Ac-CGVRPLK-BHQ3rrrrr)-retention time 16.4 minutes; ESI+ 3173.0; Q-APP-H (Hilyte750-Ac-Ceeee[Ahx]PLGLAGrrrrrK-CONH2-QXL680)-retention time 24.42 min, ESI+ 4120.0; Q-PP-H (Hilyte750-Ac-CGVRPLK-QXL680rrrrr)-retention time 23.59 min; ESI+ 3505.0. In addition we have synthesized cleaved probes B-CP (BHQ3-K-rrrrr-LAG)-retention time 18.5 min; m/z 1873.5; Q-CP (QXL680-K-rrrrr-LAG)-retention time 24.5 min, m/z 2010.5.

Spectral Measurements

Absorbance was measured using Cary 50 (Varian Inc, Walnut Creek, CA). Fluorescence measurements were done using FluoroMax4 spectrofluorometer (Horiba Jobin Yvon, Edison, NJ). Fluorescent images were acquired using IVIS Lumina II (Caliper Life Sciences, Mountain View, CA) with excitation wavelength of 675 nm and ICG emission filter set.

MMP-2 Cleavage

The probes were cleaved using a standard procedure described in the literature[22]. Briefly, to the solution of 5 μg MMP-2 in 80 μL 50 mM TRISHCl were added 8 μL 2.5 mM p-aminophenylmercury acetate (APMA) in NaOH. The enzyme was activated for 2 hours at 37 °C, after which time 10 μL of 0.35 mM B-APP-A added. Absorbance and fluorescence measurements were done after one hour of incubation of the probe with the enzyme at r.t.

Cell studies

The human fibrosarcoma cell line HT1080 was purchased from ATCC and maintained in culture according to the instructions. For the uptake study, 2 million cells were collected and incubated with 150 μL 10 μM solution of probe in HBSS for 10 minutes. After washing them with cold PBS twice, the cells were suspended in 100 μL warm water. To the suspension were added 100 μL of the 1.5% agar solution and the resulting mixture maintained in liquid form until its use in an agar phantom for photoacoustic imaging. 50 μL of the agar cell suspension was added to each phantom well.

Phantom preparation

For the dye studies polyethylene capillaries were filled with dyes and embedded in the 0.75% agar gel. For the cell studies, wells of approximately 100 μL volume were made in the gel and filled with prepared agar cell suspension.

Supplementary Material

Refer to Web version on PubMed Central for supplementary material.

Acknowledgments

References

(1). Massoud TF, Gambhir SS. Genes Dev. 2003; 17:545. [PubMed: 12629038]

(2). Massoud TF, Gambhir SS. Trends Mol Med. 2007; 13:183. [PubMed: 17403616]

(3). Li C, Wang LV. Phys Med Biol. 2009; 54:R59. [PubMed: 19724102]

(4). Wang X, Pang Y, Ku G, Xie X, Stoica G, Wang LV. Nat Biotechnol. 2003; 21:803. [PubMed: 12808463]

(5). Ermilov SA, Khamapirad T, Conjusteau A, Leonard MH, Lacewell R, Mehta K, Miller T, Oraevsky AA. J Biomed Opt. 2009; 14:024007. [PubMed: 19405737]

(6). De la Zerda A, Zavaleta C, Keren S, Vaithilingam S, Bodapati S, Liu Z, Levi J, Smith BR, Ma TJ, Oralkan O, Cheng Z, Chen X, Dai H, Khuri-Yakub BT, Gambhir SS. Nat Nanotechnol. 2008; 3:557. [PubMed: 18772918]

(7). Lu W, Huang Q, Ku G, Wen X, Zhou M, Guzatov D, Brecht P, Su R, Oraevsky A, Wang LV, Li C. Biomaterials. 2009

(8). Pan D, Pramanik M, Senpan A, Yang X, Song KH, Scott MJ, Zhang H, Gaffney PJ, Wickline SA, Wang LV, Lanza GM. Angew Chem Int Ed Engl. 2009; 48:4170. [PubMed: 19418503]

(9). Perez JM, Josephson L, O'Loughlin T, Hogemann D, Weissleder R. Nat Biotechnol. 2002; 20:816. [PubMed: 12134166]

(10). Louie AY, Huber MM, Ahrens ET, Rothbacher U, Moats R, Jacobs RE, Fraser SE, Meade TJ. Nat Biotechnol. 2000; 18:321. [PubMed: 10700150]

(11). Bremer C, Bredow S, Mahmood U, Weissleder R, Tung CH. Radiology. 2001; 221:523. [PubMed: 11687699]

(12). Weissleder R, Tung CH, Mahmood U, Bogdanov A Jr. Nat Biotechnol. 1999; 17:375. [PubMed: 10207887]

(13). Hartman KB, Laus S, Bolskar RD, Muthupillai R, Helm L, Toth E, Merbach AE, Wilson LJ. Nano Lett. 2008; 8:415. [PubMed: 18215084]

(14). Blum G, von Degenfeld G, Merchant MJ, Blau HM, Bogyo M. Nat Chem Biol. 2007; 3:668. [PubMed: 17828252]

(15). Li L, Zhang HF, Zemp RJ, Maslov K, Wang L. J Innov Opt Health Sci. 2008; 1:207. [PubMed: 19946613]

(16). Oh JT, Li ML, Zhang HF, Maslov K, Stoica G, Wang LV. J Biomed Opt. 2006; 11:34032. [PubMed: 16822081]

(17). Hu S, Maslov K, Tsytsarev V, Wang LV. J Biomed Opt. 2009; 14:040503. [PubMed: 19725708]

(18). Zhang HF, Maslov K, Stoica G, Wang LV. Nat Biotechnol. 2006; 24:848. [PubMed: 16823374]

(19). Libra M, Scalisi A, Vella N, Clementi S, Sorio R, Stivala F, Spandidos DA, Mazzarino C. Int J Oncol. 2009; 34:897. [PubMed: 19287946]

(20). Turpeenniemi-Hujanen T. Biochimie. 2005; 87:287. [PubMed: 15781315]

(21). Olson ES, Aguilera TA, Jiang T, Ellies LG, Nguyen QT, Wong EH, Gross LA, Tsien RY. Integr Biol (Camb). 2009; 1:382. [PubMed: 20023745]

(22). Jiang T, Olson ES, Nguyen QT, Roy M, Jennings PA, Tsien RY. Proc Natl Acad Sci U S A. 2004; 101:17867. [PubMed: 15601762]

(23). Zhang Y, So MK, Rao J. Nano Lett. 2006; 6:1988. [PubMed: 16968013]

(24). Goun EA, Pillow TH, Jones LR, Rothbard JB, Wender PA. Chembiochem. 2006; 7:1497. [PubMed: 16972294]

(25). Boguta A, Wrobel D. J Fluoresc. 2001; 11:129.

(26). Buschmann V, Weston KD, Sauer M. Bioconjug Chem. 2003; 14:195. [PubMed: 12526709]

(27). Larina IV, Larin KV, Esenaliev RO. J Phys D Appl Phys. 2005; 38:2633.

(28). [Accessed on May 10th, 2010]. www.biosearchtechnologies.com;www.invitrogen.com;www.anaspec.com;www.gelifesciences.com

(29). Johansson MK, Fidder H, Dick D, Cook RM. J Am Chem Soc. 2002; 124:6950. [PubMed: 12059218]

(30). Packard BZ, Komoriya A, Toptygin DD, Brand L. Journal of Physical Chemistry B. 1997; 101:5070.

(31). Packard BZ, Toptygin DD, Komoriya A, Brand L. Journal of Physical Chemistry B. 1998; 102:752.

(32). Ogawa M, Kosaka N, Choyke PL, Kobayashi H. ACS Chem Biol. 2009; 4:535. [PubMed: 19480464]

(33). West W, Pearce S. J Phys Chem-Us. 1965; 69:1894.

(34). Aguilera TA, Olson ES, Timmers MM, Jiang T, Tsien RY. Integr Biol (Camb). 2009; 1:371. [PubMed: 20023744]

(35). Stetler-Stevenson WG, Krutzsch HC, Wacher MP, Margulies IM, Liotta LA. J Biol Chem. 1989; 264:1353. [PubMed: 2536363]

(36). Springman EB, Angleton EL, Birkedal-Hansen H, Van Wart HE. Proc Natl Acad Sci U S A. 1990; 87:364. [PubMed: 2153297]

(37). Ma R, Taruttis A, Ntziachristos V, Razansky D. Opt Express. 2009; 17:21414. [PubMed: 19997381]

(38). Razansky D, Vinegoni C, Ntziachristos V. Opt Lett. 2007; 32:2891. [PubMed: 17909608]
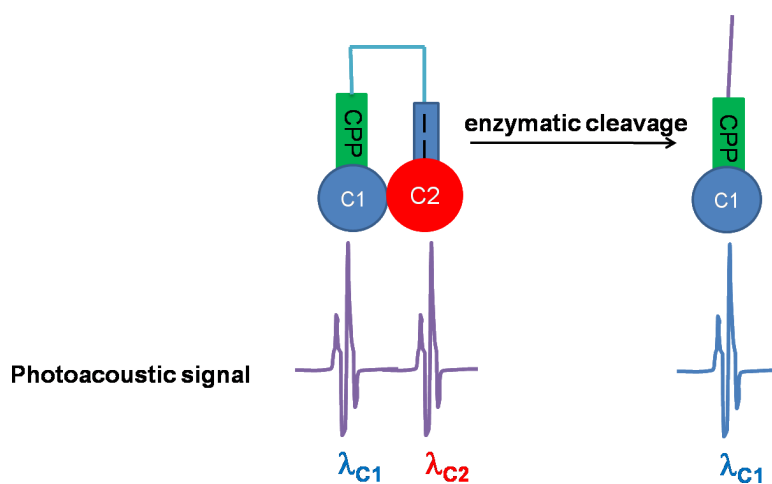
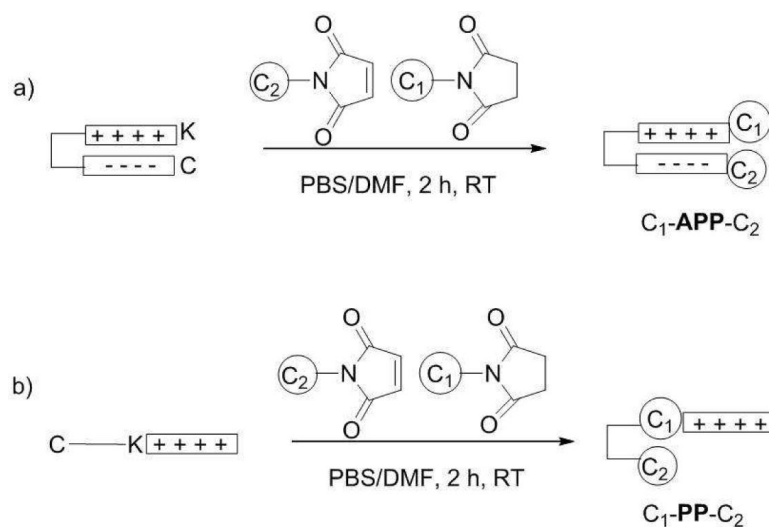**Figure 1.**
Scheme illustrating probe design. In its intact state, the probe produces a photoacoustic signal at two wavelengths (λC1, λC2) corresponding to the absorption maxima of the two chromophores C1 and C2. When cleaved by the appropriate enzyme, cell penetrating peptide (CPP) portion of the probe, carrying one of the chromophores, accumulates in cells and results in a photoacoustic signal at only one of the two wavelengths.
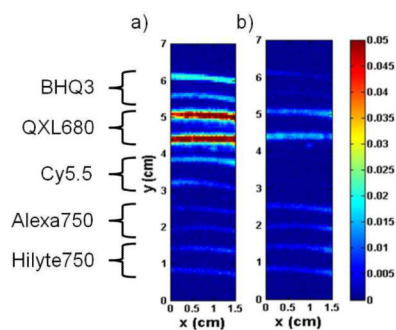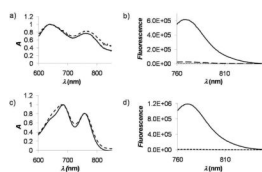
Figure 2.
Photoacoustic imaging of the chromophores. Polyethylene capillaries were filled with 10 μM solution of various dyes and imaged at 675 nm (a) and 750 nm (b). The samples were done in duplicate. The first two dyes are quenchers, BHQ3 (λabs 672 nm) and QXL680 (λabs 680 nm) while the other three are fluorophores, Cy5.5 (λabs/em 675 nm/694 nm), Alexa750 (λabs/em 750 nm/780 nm) and Hilyte750 (λabs/em 750 nm/782 nm). Color bar represent relative photoacoustic signal and corresponds to both (a) and (b). x and y represent vertical and horizontal length of the area of the agar that was scanned.
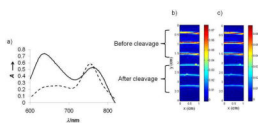
Figure 3.
One step synthesis of the photoacoustic probes. (a) Two probes were synthesized with ACPP platform, Ceeee[Ahx]PLGLAGrrrrrK: one where C1=BHQ3 and C2=Alexa750 (B-APP-A) and the other where C1=QXL680 and C2=Hilyte750 (Q-APP-H). Two other probes, B-PP-A and Q-PP-H had the same combination of the dyes but a different peptide platform, CGVRPLKrrrrr (b). The small letters signify D-amino acids. The structures of Alexa750 and Hilyte750 are proprietary information and are therefore not shown here.
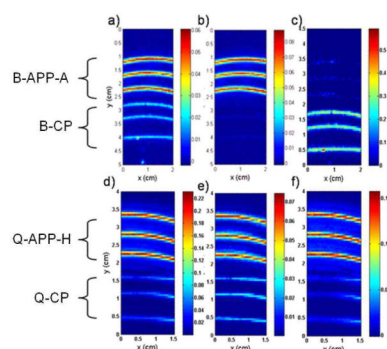
Figure 4.
(a) Normalized absorbance spectra for B-APP-A (solid line) and B-PP-A (dashed line). (b) Fluorescence spectra (λ_{ex} 745 nm) for 0.7 μM PBS solutions of Alexa750 (solid line), B-APP-A (dashed line) and B-PP-A (dotted line). The absorbance intensity at 750 nm was the same for all three probes. (c) Normalized absorbance spectra for Q-APP-H (solid line) and Q-PP-H (dashed line). (d) Fluorescence spectra (λ_{ex} 745 nm) for 0.6 μM PBS solutions of Hilyte750 (solid line), Q-APP-H (dashed line) and Q-PP-H (dotted line). The absorbance intensity at 750 nm was the same for all three probes. Please note that due to the overlap of dashed and dotted line, dotted line is not seen.
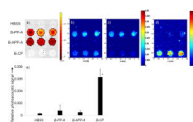
Figure 5.
Enzymatic cleavage of the photoacoustic smart probes. (a) Absorbance spectra of B-APP-A before (solid line) and after cleavage (dashed line) by the MMP-2 enzyme. Photoacoustic imaging of the probe before and after enzymatic cleavage was performed at two wavelengths, 675 nm (b) and 750 nm (c). Color bar represent relative photoacoustic signal intensity and correspond to both (b) and (c). x and y represent vertical and horizontal length of the area of the agar that was scanned. Fluorescence measurements before and after the cleavage are available in the Supporting Information.

Figure 6.
Two wavelength photoacoustic imaging of the smart probes. Photoacoustic image of 1 μM solutions of B-APP-A and B-CP (BHQ3-K-rrrrr-LAG) at 675 nm (a) and 750 nm (b). The subtraction of the normalized images taken at 675 nm and 750 nm shows clear signal for the cleaved probe (c). Photoacoustic images for 8 μM solution of Q-APP-H and Q-CP (QXL680-K-rrrrr-LAG) taken at 675 nm (d) and 750 nm (e). Subtraction of the images shows drop in the signal for Q-CP probe (f). Color bars represent relative photoacoustic signal intensity. x and y represent vertical and horizontal length of the area of the agar that was scanned.

Figure 7.
Photoacoustic imaging of the smart probe accumulation in cells. HT1080 cells were incubated with 150 μL of 10 μM solution of B-PP-A, B-APP-A or B-CP for 10 minutes and embedded in triplicate in an agar phantom. Fluorescence image (λ_{ex} 675 nm, ICG emission filter) of the agar phantom shows location of the cells as well as the uptake of B-PP-A and B-APP-A (a). The uptake of B-PP-A is higher than the one of B-APP-A, because B-PP-A lacks the polyglutamic acid part that diminishes the cell membrane transduction efficiency of the polyarginine chain. Photoacoustic images of the agar phantom with embedded cells taken at two wavelengths: 675 nm (b) and 750 nm (c). Subtraction of the images taken at 675 nm and 750 nm resulted in an image with distinct signal coming from the cells incubated with the cleaved probe (d). The accumulation of different probes in the cells was quantified from the subtraction image using mean photoacoustic values for each well (e). Error bars represent the standard error of the mean of triplicates. Accumulation of BHQ3-CPP probe was significantly different ($p < 0.05$) from the accumulation of both B-APP-A and B-PP-A. Color bars represent relative photoacoustic signal intensity. x and y represent vertical and horizontal length of the area of the agar that was scanned.

Table 1

Company reported values for extinction coefficients (ε), fluorescence quantum yields (Φ) and maximum extinction/emission wavelengths for the chromophores tested in this study[28].

Chromophore	$\lambda_{ex/em}$ (nm)	ε (mol/cm g)	Φ (%)
BHQ3	672	42,700	/
QXL680	680	110,000	/
Cy5.5	675/695	250,000	0.23
Alexa750	750/780	240,000	0.12
Hilyte750	750/780	275,000	0.12